68–14%. After that, their data have good agreement with Eq. (3). Also, Eq. (3) is greater than the data of Smith and Kuethe[12] [the maximum difference is 21% at $a(x/M)^{0.4} = 2$]. Equation (3) shows that the freestream turbulence can increases by 49%, when the porosity changes from 0.55 to 0.77.

One of the applications of this investigation is external forced convection heat transfer from a body shape inside a wind tunnel. Consider a flat plate with length L behind a woven screen with mesh spacing M. The leading edge of the flat plate is at x_a from the screen, and the end is at x_b, $x_b = x_a + L$. The Tu at both x_a and x_b can be determined from Eq. (3) and will show a decrease in Tu along the plate. It is recommended that the best value of Tu for heat transfer along the flat plate or other body shapes can be estimated using the harmonic average value of Tu, i.e.,

$$Tu = \sqrt{Tu_{x_a} \cdot Tu_{x_b}} \tag{6}$$

Summary and Conclusions

The effect of screens on wind-tunnel turbulence was examined in this study from different aspects, such as the effect of Reynolds number, screen porosity, and screen location. Furthermore, the present study developed a model to predict the turbulence intensity, based on experimental data, as a function of porosity and downstream distance. Also, this investigation found that there is no significant effect of Re_d on Tu, for the practical wind-tunnel range of $200 < Re_d < 3000$.

Acknowledgments

The second author acknowledges the financial support of the Natural Sciences and Engineering Research Council of Canada under Grant University of Waterloo 6078. The authors wish to thank M. M. Yovanovich of the University of Waterloo, Ontario, and F. Spaid at McDonnell Douglas Aerospace, St. Louis, Missouri, for their valuable discussions.

References

[1]Roach, P. E., "The Generation of Nearly Isotropic Turbulence by Means of Grids," *International Journal of Heat and Fluid Flow*, Vol. 8, No. 1, 1987, pp. 82–92.

[2]Laws, E. M., and Livesey, J. L., "Flow Through Screens," *Annual Review of Fluid Mechanics*, Vol. 10, 1978, pp. 247–266.

[3]Gad-el-Hak, M., and Corrsin, M., "Measurements of the Nearly Isotropic Turbulence Behind a Uniform Jet Grid," *Journal of Fluid Mechanics*, Vol. 62, 1974, pp. 115–143.

[4]Batchelor, G. K., and Townsend, A. A., "Decay of Isotropic Turbulence in the Initial Period," *Proceedings of the Royal Society A.*, Vol. 193, 1947, pp. 538–554.

[5]Comte-Bellot, G., and Corrsin, S., "The Use of a Contraction to Improve the Isotropy of Grid-Generated Turbulence," *Journal of Fluid Mechanics*, Vol. 25, 1966, pp. 657–662.

[6]Brundrett, E., "Prediction of Pressure Drop for Incompressible Flow Through Screens," *Journal of Fluids Engineering*, Vol. 115, No. 2, 1993, pp. 239–242.

[7]Kestin, J., Maeder, P. F., and Wang, H. E., "Influence of Turbulence on the Transfer of Heat from Plates with and without a Pressure Gradient," *International Journal of Heat and Mass Transfer*, Vol. 3, No. 1, 1961, pp. 133–154.

[8]Raithby, G., "The Effect of Turbulence and Support Position on the Heat Transfer from, and Flow Around, Spheres," Ph.D. Thesis, Univ. of Minnesota, 1967.

[9]Boulos, M., "Dynamics of Heat Transfer from Cylinders in a Turbulent Air Stream," Ph.D. Thesis, Dept. of Chemical Engineering, Univ. of Waterloo, Waterloo, ON, Canada, 1972.

[10]Tan-Atichat, J., Nagib, H. M., and Loehrke, R. I., "Interaction of Free-Stream Turbulence with Screens and Grids: a Balance Between Turbulence Scales," *Journal of Fluid Mechanics*, Vol. 144, 1982, pp. 501–528.

[11]Groth, J., and Johansson, A. V., "Turbulence Reduction by Screens," *Journal of Fluid Mechanics*, Vol. 197, 1988, pp. 139–155.

[12]Smith, M. C., and Kuethe, A., "Effects of Turbulence on Laminar Skin Friction and Heat Transfer," *Physics of Fluids*, Vol. 9, No. 12, 1966, pp. 2337–2344.

Efficient Design Constraint Accounting for Mistuning Effects in Engine Rotors

Durbha V. Murthy*
University of Toledo, Toledo, Ohio 44135
and
Christophe Pierre† and Gísli Óttarsson‡
University of Michigan, Ann Arbor, Michigan 48109

Introduction

NEARLY all design and dynamic analysis procedures for engine blades are based on the assumption that all blades on a rotor are identical. This assumption of perfect cyclic symmetry is only approximately true in practice. Small differences in blade properties, commonly referred to as mistuning, are unavoidable because they arise from manufacturing tolerances and in-service degradation. The implicit assumption in most of the design procedures in that mistuning does not significantly affect the vibratory response of the blades.

That this assumption could be wrong has been demonstrated by several studies in which the influence of small levels of mistuning on blade assembly dynamics was investigated.[1] The adverse effects of mistuning on forced response can be drastic, possibly resulting in several hundred percent increases in the blade amplitudes. In such cases, the tuned rotor assumption gives highly misleading results. This sensitivity to mistuning can be particularly dangerous when automated design optimization procedures are employed. An optimal design that is extremely sensitive to mistuning may result, invalidating the optimization process.

An obvious approach to account for the effects of mistuning is to model a mistuned rotor and place constraints on blade amplitudes. However, it is then no longer sufficient to model a single blade, leading to large increases in analysis time. Also, the actual mistuning pattern is not available until the manufacture of the rotor is complete, and mistuning differs from rotor to rotor. Furthermore, the mistuning that results from in-service degradation cannot be modeled deterministically. Thus, even a full-scale mistuned analysis cannot be usefully performed in a deterministic manner.

In this Note, we suggest a way out of this impasse. Our approach is based on the realization that the tuned rotor assumption, in spite of its limitations, is valuable in analyses and optimization procedures because of the associated analytical simplifications and computational advantages. We present a strategy to develop a constraint that restricts the sensitivity of a design to mistuning. We illustrate the approach by applying it to a popular bladed-disk model. The proposed constraint is dependent on the properties of only the tuned system, so a mistuned system analysis is not needed. A statistical model of mistuning is chosen, and so no knowledge of the actual mistuning pattern is needed. The statistics of mistuning can be estimated for a population of manufactured rotors. In addition, the time-consuming mistuned system analysis is avoided by employing perturbation theory. The proposed constraint in also easy to differentiate provided a sensitivity analysis of the tuned assembly is available, making it suitable for the computation-intensive optimization of engine

Presented as Paper 92-4711 at the AIAA/USAF/NASA/OAI Symposium on Multidisciplinary Analysis and Optimization, Cleveland, OH, Sept. 21–23, 1992; received Oct. 22, 1993; revision received July 15, 1994; accepted for publication July 18, 1994.

*Senior Research Associate, Department of Mechanical Engineering; also Resident Research Associate, Structures Division, NASA Lewis Research Center. Senior Member AIAA.

†Associate Professor, Department of Mechanical Engineering and Applied Mechanics. Member AIAA.

‡Graduate Research Assistant, Department of Mechanical Engineering and Applied Mechanics. Member AIAA.

rotors. The principal limitation is that aerodynamic coupling is not accounted for, but this may be removed by further work.

Mistuning and Vibration Localization

A well-known consequence of the tuned rotor assumption is that all blades vibrate with identical amplitudes when subjected to a cyclically symmetric excitation. This amplitude pattern is generally the designer's goal, as it minimizes fatigue. Blade mistuning destroys cyclic symmetry and thus results in blade-to-blade differences in amplitudes. If mistuning is sufficiently small, then all or most blades still participate in the vibration. However, if the level of mistuning is sufficiently high, there can be a drastic change and vibration is constrained to very few blades of the rotor, in a phenomenon known was mode localization, as depicted in Fig. 1. All of the excitation energy is then absorbed by a small number of blades, which possibly experience high amplitudes. Note that the localization phenomenon can never be predicted by tuned system analyses. Thus, a design optimized using a tuned system model could possibly have much shorter life than anticipated.

The strength of vibration localization at a given frequency is determined by the sensitivity of the response to blade mistuning at that frequency. In general, this sensitivity is a function of the nominal characteristics of the system. Next, we outline a strategy to constrain vibration localization in design procedures.

Mistuning Constraint

A statistical quantification of localization in the modes of free vibration is elusive due to the intricate shifting of the associated natural frequencies as the mistuning strength is varied. Hence, we examine instead the propagation of free waves in the mistuned assembly. This also gives us full control of the frequency at which we wish to study the localization.

The constraint we propose is based on the localization factor derived in Ref. 2. The bladed disk is modeled as an N-bay nearly cyclic assembly with several degrees of freedom per bay, one of which couples adjacent bays (a monocoupled system). Each bay represents one blade and one disk sector. In perfectly periodic monocoupled structures there exists only one pair of wave modes at each frequency, one traveling clockwise and one traveling counterclockwise.[3] There are bands of frequencies, known as passbands, in which these waves travel with no attenuation. Vibrations of the structure may be expressed in terms of these wave modes through a 2×2 wave transfer matrix relating wave mode amplitudes at adjacent bays. For a tuned assembly the wave transfer matrix is diagonal since clockwise and counterclockwise traveling waves are independent.

In a mistuned blade assembly, however, the wave transfer matrix is not diagonal. A possibility of localization (standing wave) exists even in the frequency passbands, because wave modes can no longer travel unattenuated through the structure. Instead a wave is partially reflected as it traverses each boundary between the dissimilar bays. A left incident wave to the structure, L_{N+1}, is partially reflected as it passes through the N bays, and the emergent wave is equal to $L_1 = t_N L_{N+1}$, where t_N is the transmission coefficient for the N-bay structure at that frequency. Note that, in this cyclic model, the emergent wave adds to the incident wave after each revolution around the assembly. This superposition effect is, however, insignificant for large localization effects.

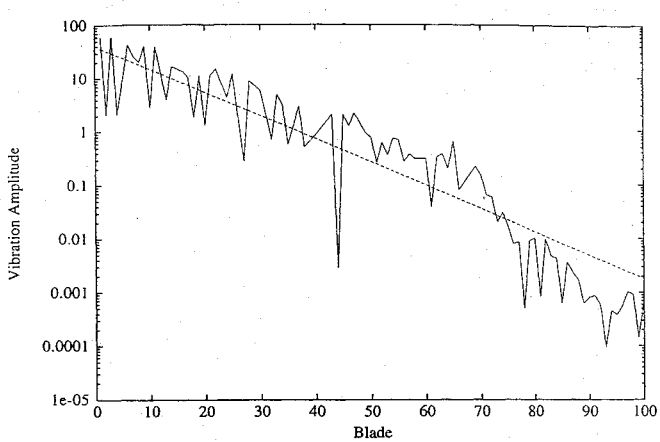

Fig. 1 Typical vibration amplitude pattern for a randomly mistuned 100-blade assembly with localization factor $\gamma = 0.1$. The asymptotic, or average, exponential decay is also shown (- - -).

Using now the conjecture[2] that, on average, the ratio of emergent to incident wave amplitude decreases exponentially as N increases, we define a frequency-dependent localization factor γ as the asymptotic rate of decay of the wave amplitude transmitted through the N-bay system:

$$\frac{L_{N+1}}{L_1} \sim e^{-\gamma N} \quad \text{as} \quad N \to \infty \tag{1}$$

Equivalently, assuming spatial self-averaging, one has

$$\gamma = \left\langle \frac{1}{N} \ell_n \left| \frac{1}{t_N} \right| \right\rangle \tag{2}$$

where $\langle \bullet \rangle$ denotes an average. Averaging, or equivalently, taking the asymptotic limit, is used to eliminate explicit dependence on the mistuning pattern. Note that the localization factor defines the average exponential decay rate per bay and is thus a descriptor of the strength of localization.

Next, we illustrate the significance of the localization factor. Recall that the decay of a wave propagating through the structure is governed by $e^{-\gamma N}$. For $\gamma = 0.1$, the ratio of the amplitudes at adjacent bays is $e^{-0.1} \simeq 0.90$, such that on average the energy transmitted from one blade to the next is 82%, and 56% is transmitted to the third blade. The amplitude would be attenuated by 90% by the 24th blade. Figure 1 depicts the amplitude pattern for a wave subject to localization with $\gamma = 0.1$. For $\gamma = 1$ the average energy transmitted to the next blade is 13.5%, and less than 0.25% of the energy reaches the third blade! In comparison, for the tuned undamped system $\gamma = 0$, and 100% of the energy is transmitted.

From Fig. 1, we see that the significance of the value of γ depends on the size of the assembly, and to be meaningful the localization factor must be used in conjunction with the number of blades, N. Obviously the localization in Fig. 1 would appear much less significant in a 10-bay assembly than in a 100-bay assembly. In the former case $\gamma N = 1$ but $\gamma N = 10$ in the latter. This suggests constraining γN to a suitable value to limit the effects of localization in a mistuned blade assembly. For instance, one might require a wave propagating through the system to retain at least 80% of its amplitude, on average, thus:

$$e^{-\gamma N} \geq 0.8 \quad \text{or} \quad \gamma N + \ell_n 0.8 \leq 0 \tag{3}$$

The evaluation of the constraint, Eq. (3), requires the calculation of the localization factor. An obvious but costly solution is to evaluate γ with a Monte Carlo simulation. In this "brute force" approach, the localization factor is the average of the decay rates for multiple realizations of mistuned assemblies generated randomly. The method is expensive due to the high number of realizations usually required for adequate accuracy. Its cost is compounded by the fact that the localization factor must be obtained at all frequencies of interest. An alternative to Monte Carlo simulations is an analytical approximation of γ via perturbation techniques.[2] We illustrate this approach in the next section.

Illustration

The previous concepts are applied to a common bladed-disk model[2] (see Fig. 2). It features two degrees of freedom per bay: one for the single-mode motion of the blade and one for motion of the disk at the blade root, denoted q_i^b and q_i^d, respectively. Corresponding to q_i^b are the blade modal mass m_b and modal stiffness k_b^i. The mass m_d simulates the effective mass of the blade root and the corresponding section of the disk. The stiffness k_d represents the basic stiffness of the root disk, and k_c provides the disk coupling between adjacent blades. We assume that mistuning affects only

the blade stiffness k_b^i. The following dimensionless parameters are introduced:

$$\bar{k}_d = k_d/k_b; \qquad \bar{k}_c = k_c/k_b; \qquad \bar{k}_b^i = k_b^i/k_b$$
$$\bar{m} = m_d/m_b; \qquad \bar{\omega} = \omega/\sqrt{k_b/m_b} \tag{4}$$

where k_b is the average value of k_b^i.

The distribution of free vibration natural frequencies is plotted in Fig. 3 against the number of nodal diameters in the corresponding mode of vibration, for $\bar{k}_d = 10$, $\bar{k}_c = 1$, and $\bar{m} = 10$. There are two frequency bands because our model has two degrees of freedom per bay. Note that even quite complicated bladed-disk models can be reduced to the model in Fig. 2 by fitting the actual natural frequency distribution to that shown in Fig. 3 and identifying the values of $\bar{k}_d$, $\bar{k}_c$, and $\bar{m}$ for best fit.

Recall that since γ is a function of frequency, the localization strength differs for each rotor mode. However, in an optimization procedure, it would be too cumbersome to place constraints on the localization factors for each mode. Any typical or "interesting" mode can be chosen for this purpose. For convenience, the mode corresponding to an interblade phase angle of $\pi/2$ (with $N/4$ nodal diameter) is suggested. Note that the frequency corresponding to this mode is the median natural frequency, and in that sense this mode may be considered typical. The localization factor of the system can then be written as[2]

$$\gamma = \begin{cases} \dfrac{S^2 s^2}{8} & \text{for small } S \\ \ell n(Ss\sqrt{3}) - 1 & \text{for large } S \end{cases} \tag{5}$$

where s is the standard deviation of mistuning in blade stiffness, and S is a sensitivity measure defined by[2]

$$S = \frac{1}{4\bar{k}_c}\Big[2\bar{k}_c + \bar{k}_d - \bar{m} - 1 \mp \sqrt{(2\bar{k}_c + \bar{k}_d + \bar{m} + 1)^2 - 4\bar{m}(\bar{k}_d + 2\bar{k}_c)}\Big]^2 \tag{6}$$

where the minus sign refers to the first frequency band and the plus to the second. Note that Eq. (5) gives γ as a discontinuous function of the system parameters. This potential limitation in optimization applications could be overcome by redefining γ using a spline interpolation between the two segments of Eq. (5). Results from Monte Carlo simulations, if available, can be used to insure accurate interpolation.

The constraint on the influence of mistuning, Eq. (3), can now be expressed in terms of the tuned model parameters and the mistuning strength.

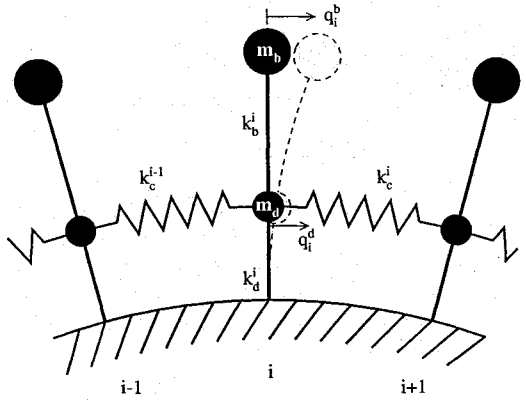

Fig. 2 The *i*th blade in an *N*-blade assembly with one blade coordinate and one disk coordinate per bay is shown with its two coupled adjacent blades.

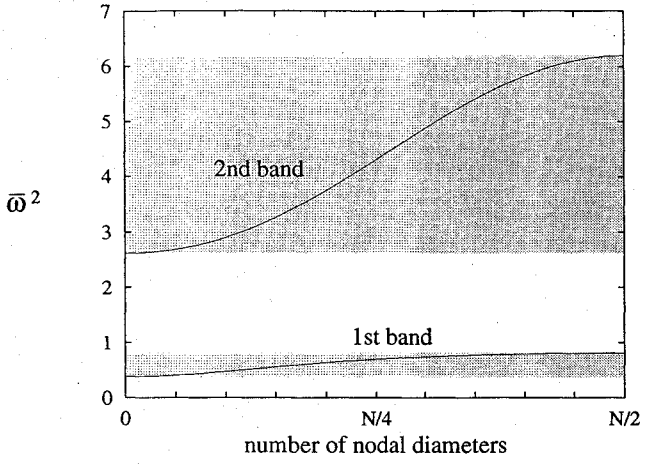

Fig. 3 Natural frequencies as a function of nodal diameter for the bladed-disk model in Fig. 2.

Acknowledgments

This work was supported by the Structural Dynamics and the Launch Vehicle Technology Branches and the Institute for Computational Mechanics in Propulsion at NASA Lewis Research Center (Grants NAG3-742 and NAG3-1163). George Stefko was the technical monitor.

References

[1]Pierre, C., and Murthy, D. V., "Aeroelastic Modal Characteristics of Mistuned Blade Assemblies: Mode Localization and Loss of Eigenstructure," *AIAA Journal*, Vol. 30, No. 10, 1992, pp. 2483–2496.

[2]Óttarsson, G., and Pierre, C., "A Transfer Matrix Approach to Vibration Localization in Mistuned Blade Assemblies," International Gas Turbine Conference, ASME Paper 93-GT-115, Cincinnati, OH, May 1993.

[3]Mead, D. J., "Wave Propagation and Natural Modes in Periodic Systems, I: Mono-Coupled Systems," *Journal of Sound and Vibration*, Vol. 40, 1975, pp. 1–18.

Buckling of Polygonal and Circular Sandwich Plates

C. M. Wang*
National University of Singapore, Kent Ridge 0511, Singapore

Introduction

SANDWICH plates are extensively used in aerospace structures. When used in such structures, these plates are often subjected to in-plane forces. Thus, it is important to understand the buckling behavior of sandwich plates under in-plane forces.

Since the lighter core of the sandwich is usually relatively thick and low in stiffness when compared to isotropic plates, the effect of transverse shear deformation becomes significant and, thus, cannot be neglected in the buckling analysis. Otherwise, the buckling load will be overpredicted. A simple plate theory which allows for the effect of shear deformation was proposed by Reissner[1] for bending, and it was later extended to vibration and buckling problems by Mindlin[2] and Kollbrunner and Herrmann.[3] The theory assumes linear variations of the in-plane displacements through the thickness. Although the assumption gives rise to constant values of transverse shear stress distributions through the thickness (violating the condition of vanishing shear stresses at the surfaces), it has been found to produce reasonably accurate eigenvalue solutions by employing shear correction factors on the transverse shear modulii. This first-order shear deformation theory will be adopted for the buckling analysis of sandwich plates.

Received March 7, 1994; revision received Aug. 4, 1994; accepted for publication Aug. 13, 1994.

*Senior Lecturer, Department of Civil Engineering.